Table 1. X-ray powder diffraction data for the high-pressure form of InTe (Mn-filtered FeKα radiation, 57.3-mm camera).

hkl	$d_{obs.}$ Å	$I_{obs.}$ *	$I_{calc.}$ †
200	3.07	100	100
220	2.17	80	74
222	1.77	25	24
400	1.53	15	13
420	1.37	45	37
422	1.254	35	34
440	1.086	20	19
442, 600	1.024	50	69

* $I_{obs.}$ = visually estimated relative intensities. † $I_{calc.}$ = calculated relative intensities for InTe with the NaCl structure.

with those given for tetragonal InTe by Darnell, Yencha, and Libby (*5*) and by Schubert, Dörre, and Kluge (*12*). We conclude that the high-pressure cubic form of InTe has the NaCl (type B1) structure.

The cell edge of our metallic InTe is 6.160 ± 0.005 Å based on x-ray powder diffraction data, obtained with V-filtered CrKα radiation and a 57.3-mm camera, extrapolated to $\theta = 90°$ from the function

$$\frac{1}{2}\left(\frac{\cos^2\theta}{\sin\theta} + \frac{\cos^2\theta}{\theta}\right)$$

The corresponding calculated density of metallic InTe is 6.887 g/cm^3. The measured density determined pycnometrically was 6.84 g/cm^3. The density increase relative to the low-pressure tetragonal form (*12*) is 15.6 percent. The interatomic distance In-Te is 3.08 Å. The sum of the single-bond metallic radii given by Pauling (*13*) for In (1.42 Å) and Te (1.37 Å) is 2.79 Å. This distance may be corrected for sixfold coordination of In and Te by using Pauling's valence of 2 for metallic tellurium and the relationship $D(n = \frac{1}{3}) = D(n = 1) - 0.6 \log n$, where D is the interatomic distance and n is the bond number (*13*). The corrected value is 3.08 Å in exact agreement with the experimental value.

Schubert *et al.* (*12*) showed that the low-pressure tetragonal form of InTe has the TeSe (type B37) structure, in which half the indium atoms are tetrahedrally coordinated and half are hexahedrally coordinated with tellurium. The high-pressure phase transition in InTe, therefore, involves a reconstructive transformation of first coordination in which the coordination of indium with respect to tellurium changes from 4 and 8 to 6.

On a pressure-temperature-composition equilibrium diagram of the InSb-InTe system, the stability region for the phase with the NaCl structure must be bounded by a curved surface which intersects the *P-T* plane in a straight line between 13 kb at 700°C and 32 kb at 0°C (*14*), and intersects the *T-X* plane at the composition (InSb·3 InTe).

After this paper was submitted for publication, the contribution of Banus *et al.* (*14*) appeared. Our findings regarding preparation of metallic InTe without subambient quenching and our conclusion that it has the NaCl structure are in complete agreement with their work (*14*). We do not agree with their statement that the x-ray data of Darnell *et al.* (*5*) can be interpreted as having the CsCl structure, because the intensities are wholly incompatible with this structure. Furthermore, it is impossible for InTe to have the CsCl structure with a cell edge of 3.07 Å and one formula weight per cell, giving a calculated density of 13.8 g/cm^3 as discussed by Banus *et al.* (*14*), because the (100) reflection for InTe with the CsCl structure would approach zero intensity whereas the reflection at 3.07 Å is the strongest line of the cubic InTe pattern. Banus *et al.* (*14*) use SnTe as an example of an analogous compound whose structure is "known" to be that of NaCl. Whether SnTe has a simple cubic or the NaCl structure, however, is as equivocal as the arguments regarding the structure of metallic InTe because of the essentially equivalent x-ray scattering power of Sn and Te. The x-ray data for both compounds are compatible with either a simple cubic or NaCl structure. Because of the existence of high-pressure forms of InAs and InP, which reportedly have the NaCl structure (*4*, *7*) presumably on the basis of observed reflections with all indices odd, we conclude that the weight of evidence favors the NaCl (Bl) structure for metallic InTe.

C. B. SCLAR
L. C. CARRISON
C. M. SCHWARTZ
Battelle Memorial Institute, Columbus 1, Ohio

References and Notes

1. H. A. Gebbie, P. L. Smith, I. G. Austin, J. H. King, *Nature* **188**, 1095 (1960); A. Jayaraman, R. C. Newton, G. C. Kennedy, *ibid.* **191**, 1288 (1961); P. L. Smith, J. H. King, H. A. Gebbie, in *Physics and Chemistry of High Pressures* (Gordon and Breach, New York, 1963), pp. 140–142.
2. M. D. Banus, R. E. Hanneman, A. N. Mariano, E. P. Warekois, H. C. Gatos, J. A. Kafalas, *Appl. Phys. Letters* **2**, 35 (1963).
3. P. L. Smith and J. E. Martin, *Nature* **196**, 762 (1962); A. J. Darnell and W. F. Libby, *Science* **139**, 1301 (1963).
4. J. C. Jamieson, *Science* **139**, 845 (1963).
5. A. J. Darnell, A. J. Yencha, W. F. Libby, *ibid.* **141**, (1963).
6. H. T. Hall, *Rev. Sci. Instr.* **31**, 125 (1960); C. B. Sclar, L. C. Carrison, C. M. Schwartz, in *High Pressure Measurement*, A. A. Giardini and E. C. Lloyd, Eds. (Butterworth, Washington, D.C., 1963), pp. 286–300.
7. S. Minomura and H. G. Drickamer, *J. Phys. Chem. Solids* **23**, 451 (1962).
8. J. D. H. Donnay *et al.*, *Crystal Data*, Am. Crystallog. Assoc. Monograph No. 5 (1963).
9. G. Hägg and A. G. Hybinette, *Phil. Mag.* **20**, 913 (1935).
10. N. A. Goryunova, S. I. Radautsan, G. A. Kiosse, *Fiz. Tver. Tela* **1**, 1858 (1959).
11. H. E. Swanson, R. K. Fuyat, G. M. Ugrinic, *Natl. Bur. Stand. U.S. Circ. No. 539* **IV**, 73 (1955).
12. J. Schubert, E. Dörre, M. Kluge, *Z. Metallkunde* **46**, 216 (1955).
13. L. Pauling, *The Nature of the Chemical Bond.* (Cornell Univ. Press, Ithaca, ed. 3, 1960), p. 400, Table 11-1.
14. M. D. Banus, R. E. Hanneman, M. Strongin, K. Gooen, *Science* **142**, 662 (1963).
15. We thank D. A. Vaughan and A. E. Austin for critical comments on the crystal structure of metallic InTe.

14 October 1963

Cretaceous Fossils Collected at Johnson Nunatak, Antarctica

Abstract. *Sandstone samples collected at 74°52′S, 74°02′W have been assigned a Cretaceous age on the basis of a faunal assemblage including* Rotularia callosa (*Stoliczka*).

Rock specimens were collected at 11 locations on the Antarctic Peninsula Traverse, 1961–62 (*1*). At one location, Johnson Nunatak (*2*), located at 74°52′S, 74°02′W, samples of a fossiliferous marine sandstone were

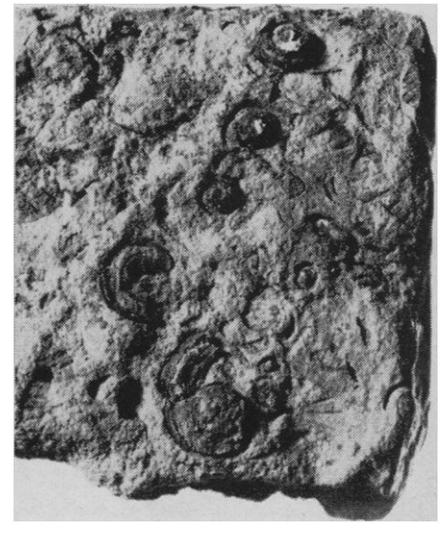

Fig. 1. *Rotularia callosa* (Stoliczka) fossils from Johnson Nunatak (1.6 times natural size).

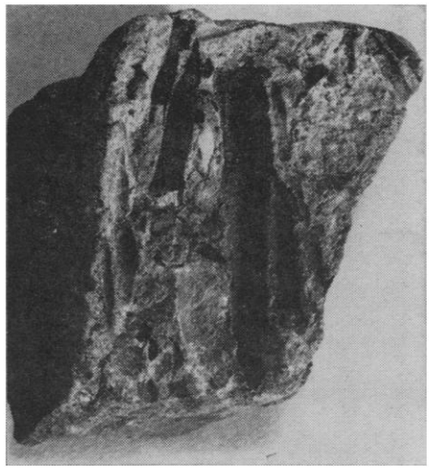

Fig. 2. *Belemnoid* fossil casts from Johnson Nunatak (0.6 times natural size).

collected. A Cretaceous age for this bed was based on the following assemblage:

Rotularia callosa (Stoliczka), a serpulid worm species (Fig. 1).
Belemnoid (Fig. 2).
Synclyclonema sp., a pelecypod.
Variamusium? sp., a pelecypod.

Rotularia callosa occurs frequently in Cretaceous rocks of the Southern Hemisphere, having previously been described from the Aptian of Patagonia and the Campanian of New Zealand as well as from the Cenomanian of India (*3*).

In Antarctica this species has been reported from beds of Aptian age on Alexander I Island (71°21′S, 68°21′W) and from beds of Campanian age on James Ross and Snow Hill islands (64°S, 58°W) (*3*). No fossils present at Johnson Nunatak allow a more precise age than that from Aptian to Campanian indicated by *R. callosa*.

The collection was examined by N. F. Sohl (*4*) who corroborated the identifications and Cretaceous age.

JOHN C. BEHRENDT
THOMAS S. LAUDON
Geophysical and Polar Research Center, University of Wisconsin, Madison, and *Department of Geology, Wisconsin State College, Oshkosh*

References and Notes

1. J. C. Behrendt and P. E. Parks, *Science* **137**, 601 (1962); T. S. Laudon. J. C. Behrendt, N. J. Christensen, *J. Sediment. Petrol.*, in press.
2. Name proposed by field party but not officially adopted by U.S. Board of Geographic Names. U.S. Geologic Survey designation H1M.
3. H. W. Ball, *Falkland Islands Dependencies Survey Report No. 24* (1961).
4. Paleontology and Stratigraphy Branch, U.S. Geological Survey, U.S. National Museum, Washington, D.C.

18 November 1963

Equatorial Undercurrent of the Indian Ocean

Abstract. *Measurements of currents at the equator in the Indian Ocean indicate the presence of an equatorial undercurrent. This current is similar in many respects to the undercurrent in the Pacific and Atlantic oceans. The undercurrent in the Indian Ocean is located in the thermocline and is of low magnitude, unsteady, and more strongly developed on the eastern side of the ocean.*

During the past year the equatorial circulation of the Indian Ocean has been studied in two 3-month cruises carried out from the research vessel, *Argo*, of the Scripps Institution of Oceanography of the University of California. These studies are a United States contribution to the scientific program of the International Indian Ocean Expedition (*1*).

The main objective of these studies was to determine whether the Indian Ocean possesses a current structure similar to that found near the equator in the Atlantic and Pacific oceans (*2*). Measurements at the equator in these oceans have revealed high-speed, subsurface, eastward flows centered at the equator. The Equatorial Undercurrent in the Pacific (Cromwell Current) has been shown to have a maximum speed of 100 to 150 cm/sec at a depth of 50 to 100 m. The current is about 4° wide, symmetrical about the equator, and relatively steady in time. The Equatorial Undercurrent in the Atlantic, although less well documented, appears to be analogous to its counterpart in the Pacific (*3*).

It is generally believed that the Equatorial Undercurrent is in some way driven by the surface winds (*4*). If so, one might expect to find a difference in the equatorial current structure with different wind systems. For this reason, observations were made during the two phases of the Indian Ocean monsoon.

The first cruise, 28 June to 24 September 1962, was during the period of the southwest monsoon. The second cruise, 16 February to 15 May 1963, began at the end of the northeast monsoon period and concluded during the beginning of the southwest monsoon period. The results of a preliminary analysis of the data from the first cruise have already been reported (*5*). Some of the conclusions presented in that paper have now been modified upon further analysis of the data. In particular, an equatorial undercurrent structure, although somewhat different from that observed to be characteristic for the Pacific and Atlantic oceans, was measured on the eastern meridional sections of this first cruise and our conclusion that no undercurrent was present now applies only to the western sections. This report is based on the data from both cruises and is focused on the question of the existence of the Equatorial Undercurrent in the Indian Ocean. The station pattern on the two cruises was nearly identical with four north-south sections across the equator and a zonal section along the equator occupied during both periods (Fig. 1). Current measurements were made from the surface down to 400 m on each meridional section at 1° intervals from 2°N to 2°S. The measurements were made with a telemetering current meter from a drifting ship by a technique previously described by Knauss (*3*).

On three of the eight sections (79°E, 89°E, and 92°E) the distribution of the zonal component of velocity with depth was similar to that of the Equatorial Undercurrent. The core of these eastward flows was located in the middle thermocline, the maximum eastward speeds were centered at the equator, the associated meridional components were small in comparison to the zonal component, and the current structure in the thermocline was stable over periods of

Table 1. Maximum measured eastward velocity component in thermocline and associated meridional velocity component and depth for equatorial stations where the undercurrent was present. Positive meridional components are northward and negative components are southward.

Date	Zonal component (cm/sec)	Meridional component (cm/sec)	Depth (m)
	61°E		
9 March	27	+13	81
31 March	57	− 5	80
	69°E		
4 March	49	−16	90
	77°E		
1 March	31	+ 2	120
	79°E		
9 July	19	− 7	125
2 Sept.	67	+20	110
8 Sept.	61	−32	100
	85°E		
7 April	60	+23	105
	89°E		
11 Sept.	51	+12	120
17 Sept.	34	+14	140
	92°E		
9 April	81	− 7	100
22 April	76	+19	120